THE ASTROPHYSICAL JOURNAL, 272:54–67, 1983 September 1

THE RATE OF STAR FORMATION IN NORMAL DISK GALAXIES

ROBERT C. KENNICUTT, JR.
University of Minnesota, Department of Astronomy
Received 1982 October 11; accepted 1983 February 9

ABSTRACT

Photometry of the integrated Hα emission in a large sample of field spiral and irregular galaxies has been used to obtain quantitative estimates of the total star formation rate (SFR) in the galaxies. The photoionization properties of a stellar population have been modeled for a variety of choices for the initial mass function (IMF). The observed *UBV* colors and Hα emission equivalent widths place tight constraints on the slope of the IMF between 1 $M_\odot$ and 50 $M_\odot$ in the galaxies; excellent agreement with the observed galaxy colors and Hα emission is obtained with models using an IMF slope close to Salpeter's original value. The properties of late-type galaxies are not well reproduced by the Miller-Scalo solar neighborhood IMF. The extinction-corrected star formation rates are large, as high as 20 $M_\odot$ yr^{-1} in giant Sc galaxies ($H_0 = 50$ km s^{-1} Mpc^{-1}). The current rates in late-type galaxies are comparable to the past rates averaged over the age of the disk; late-type disk galaxies have evolved at a nearly constant rate, confirming earlier models by Searle, Sargent, and Bagnuolo. Little evidence is found for a strong correlation between the SFR and average gas density; if the SFR $\propto \rho^n$, then the exponent n must be much less than 1, corroborating earlier studies of star formation in the solar neighborhood by Miller, Scalo, and Twarog. Comparison of the present SFRs with the remaining supply of interstellar gas yields consumption time scales of only a few times 10^9 years in most cases, in agreement with the model estimates of Larson, Tinsley, and Caldwell. Infall of intergalactic gas may extend these time scales, but it is unlikely to replenish the gas as rapidly as it is being consumed in the late-type systems. Consequently it is possible that the present epoch is characterized by rapid changes in the integrated properties and morphologies of disk galaxies.

Subject headings: galaxies: evolution — galaxies: photometry — galaxies: stellar content — galaxies: structure — stars: formation

I. INTRODUCTION

Despite the broad application of H II regions as qualitative tracers of star formation in other galaxies, little effort has been made to exploit the potential of the ionized gas emission for providing quantitative measurements of star formation rates. In principle, at least, measurement of the integrated Balmer photon flux of a galaxy should provide a direct measurement of the Lyman continuum luminosity and the corresponding OB star formation rate (SFR) in the galaxy. In practice, however, the accurate determination of the OB SFR, and the extrapolation to a total SFR, requires careful consideration of the initial mass function (IMF) of the stellar population, the ultraviolet emission of the stars, and the effects of dust absorption on the measured Balmer fluxes.

This paper presents a first attempt at measuring total star formation rates in a large sample of disk galaxies, using recently obtained data on their integrated Hα + [N II] emission (Kennicutt and Kent 1983, hereafter Paper I). By combining the emission line data with broad-band *UBVR* photometry it is possible to place constraints on both the current SFRs and the average initial mass functions in the galaxies. The first part of the paper describes the data set, the photoionization model, and the results, along with a detailed discussion of the possible sources of uncertainty in the derived SFRs. The implications of the results for our understanding of galaxy evolution are discussed in the latter part of the paper.

II. DATA

Hα + [N II] emission line and red continuum fluxes have been measured for 170 nearby field and Virgo cluster galaxies of various types. Details of the measurements and the calibration are described in Paper I, which includes a complete listing of the data and a preliminary comparison of the emission line properties of the galaxies with other integrated properties. The final data consist of absolute integrated line fluxes, measured with a large-aperture photoelectric photometer through interference filters, and an emission-line to red-continuum flux ratio, expressed as an equivalent width. Typical equivalent widths range from zero for elliptical and S0 galaxies, to 20–50 Å for late-type spirals, to as much as 150 Å for some irregular and unusually active spiral galaxies. The observational uncertainty is typically ±2–3 Å, so that galaxies with detectable emission (usually types Sb and later) have line fluxes and equivalent widths measured to an accuracy of ~ ±10%, low enough to study the real variations in star formation activity among galaxies of a given type. (The spectro-

photometric measurements which are presented in Paper I are less precise and will not be used in this paper.)

For the photoionization and SFR calculations we need to remove any contamination of the Hα emission by nonthermal nuclear emission, underlying stellar Hα absorption, [N II] emission, or absorption by dust. A comparison of Keel's (1982) nuclear Hα + [N II] fluxes with the integrated fluxes in Paper I showed that nuclear emission is negligible ($\lesssim 5\%$) in most of the spirals studied. About 10% of the program galaxies do exhibit strong nuclear emission, either from Seyfert nuclei or narrow-lined "starburst" nuclei (Weedman *et al.* 1981), and those galaxies have been excluded from consideration in this paper. Hα absorption in the underlying red continuum should be small as well, since the light at those wavelengths is dominated by G–K giants with a typical absorption equivalent width of only 1–2 Å. Since the effects of nuclear emission and Hα absorption are both small and are of comparable (and opposite) magnitude, I have not bothered to correct the integrated fluxes for either. The uncertainty introduced is only important for early-type galaxies with weak disk emission (EW $\lesssim$ 5 Å), but for those galaxies the measurement uncertainties are dominant anyway.

Average corrections for the larger effects of [N II] emission and extinction were applied to the data set as a whole. A compilation of spectrophotometric [N II]/Hα ratios of extragalactic H II regions in Paper I showed that the average Hα/(Hα + [N II]) ratio is fairly constant in spiral and irregular galaxies, spanning the range 0.75 ± 0.12 in 14 spiral galaxies (mostly Sc's), and 0.93 ± 0.05 in seven irregulars. These average values have been applied uniformly to the galaxy sample.

Extinction is by far the most important source of systematic uncertainty in the SFR determination, whether measured from Hα as in this paper or from modeling the broad-band colors. Fortunately there exists a rapidly growing set of radio continuum data which allows us to make at least an average correction for the effects of extinction on the Hα emission. Israel and Kennicutt (1980) compared 6 cm radio continuum fluxes for 30 extragalactic H II regions with their Hα fluxes and derived an average extinction at 6563 Å of 1.3 mag. More recently, measurements of the integrated "thermal" radio fluxes of entire galaxies have been made by Israel and van der Hulst (1982) and Gioia, Gregorini, and Klein (1982). Those data are shown in Figure 1, along with the corresponding Hα + [N II] fluxes from the present work. The thermal radio emission comprises only a small fraction of the total flux, even at 10 GHz, and consequently the individual radio fluxes are highly uncertain. Nevertheless there exists a good correlation between radio and line emission. The radio fluxes are systematically higher than the predicted free-free emission of a 10,000 K gas by a factor of 2.8, implying an absorption of 1.1 mag at Hα, if the radio emission is purely thermal. This result is consistent with the Israel and Kennicutt result for individual H II regions, and will be adopted as the average correction for the Hα fluxes. The largest sources of systematic error in the correction are possible nonthermal contamination of the radio emission, which would cause us to overestimate the absorption correction, and absorption of Lyman continuum radiation by dust within the H II regions (Sarazin 1977), which would work in the opposite direction. Consequently, the overall absorption scale is uncertain, at roughly the 20–30% level.

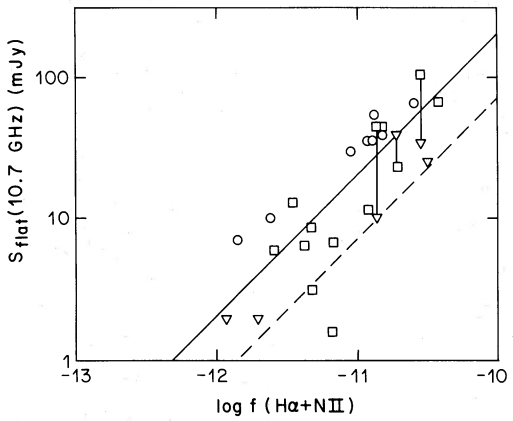

FIG. 1.—A comparison of the integrated Hα + [N II] emission line fluxes with thermal radio fluxes, as determined from multifrequency spectra by Israel and van der Hulst (*open circles*) and by Giola, Gregarini, and Klein (*boxes*). Upper limits are denoted by triangles. The solid line is a median fit (unity slope), while the dashed line is the expected relation for free-free emission.

The final Hα luminosities of the program galaxies, corrected for [N II] emission and extinction as described above (distances corresponding to $H_0 = 50$ km s^{-1} Mpc^{-1}), are listed in the Appendix (Table 1). All spiral galaxies in Paper I are listed, except those with active nuclei and Virgo Cluster members. *The individual entries in Table 1 must be treated with extreme caution*; because of the large and possibly variable extinction they are accurate at best to $\pm 50\%$. Table 1 is provided primarily to illustrate the variation in star formation properties encountered in the sample. Extinction is clearly the largest source of uncertainty in the determination of star formation rates for any single galaxy using this method; on the other hand, the average statistical properties of the sample should be considerably more accurate.

III. PHOTOIONIZATION CALCULATIONS

A modified Zanstra method is used to estimate the OB SFRs. The Hα luminosities in Table 1 were converted to Lyman continuum photon fluxes, using the simple Case B recombination conversion (Brocklehurst 1971). We shall assume implicitly that this value represents the total Lyman continuum of the OB stellar population in the galaxies—in other words, that the galaxies as a whole are Lyman radiation-bounded. This assumption is very difficult to test at present, and to the extent that some ultraviolet radiation may escape undetected in these galaxies, the reader should bear in

mind that the star formation rates derived here are technically *lower limits* to the true SFR.

The ionization requirements represented by the fluxes in Table 1 are prodigious. A typical giant Sc galaxy emits 10^{42} ergs s^{-1} in Hα, corresponding to the combined luminosities of 25,000 O5 stars. With such large numbers of ionizing stars involved, it is most proper to calculate the photoionization statistically, by computing the ultraviolet luminosities for each stellar mass on the main sequence, and weighting the individual contributions by an initial mass function.

Evolutionary tracks in the (log L_{bol}, T_{eff})-plane were compiled for stars of initial mass 8, 10, 15, 20, 25, 30, 40, 50, 60, 80, and 100 $M_\odot$, from the work of Chiosi, Nasi, and Sreenivasan (1978) and Stothers and Chin (1979). For initial masses of 30 $M_\odot$ and larger, models with moderate degrees of mass loss were used, corresponding to the Stothers and Chin Case B grid, or the Chiosi *et al.* $\alpha = 0.83$ grid. The main effect of mass loss on the ultraviolet properties of the stars is to lengthen the hydrogen-burning lifetime, and thus to slightly increase the integrated ionization per star over its lifetime. Maeder's (1980) very high mass tracks were also used to investigate the effect of extending the IMF to masses as high as 240 $M_\odot$. Solar compositions were used in all cases. Changes in composition do affect the derived Lyman luminosities and lifetimes (Balick and Sneden 1976; Stothers and Chin 1976), but the dependence is relatively weak ($N_L \propto Z^{-0.4}$ approximately).

Lyman continuum fluxes, bolometric corrections, and *UBV* colors as a function of effective temperature and gravity were taken from the model atmosphere grids of Hummer and Mihalas (1970; unblanketed NLTE) and Kurucz (1979; blanketed LTE). For temperatures above 50,000 K the LTE models of Van Citters and Morton (1970) were also used. The atmospheres and evolutionary tracks were then combined to generate curves representing the dependence of the Lyman continuum luminosity as a function of time for each initial stellar mass. Integrating each curve yields the total number of photons emitted per star over its lifetime. Since the lifetimes of these stars are short (most $< 10^7$ yr) relative to any time scale we need to consider, these are the only results we shall need here. Similar numbers representing the total radiation in *UBV* and *R* (the latter from Johnson 1966) were computed, though in most cases their contribution to the total light of the galaxy is negligible.

Model stellar populations were constructed for three choices of the IMF. The Miller-Scalo (1979) solar neighborhood IMF was used in its power-law approximation:

$$\psi(m) \propto m^{-1.4} \quad (0.1 < m < 1\ M_\odot)$$

$$\propto m^{-2.5} \quad (1 < m < 10\ M_\odot)$$

$$\propto m^{-3.3} \quad (10 < m < 100\ M_\odot)$$

The lower mass cutoff was adopted following Tinsley (1981); in any case, stars below this limit would not contribute significantly to the total mass, given the shallow IMF slope. The upper cutoff mass of 100 $M_\odot$ was adopted somewhat subjectively, on the basis of a comparison of the observed H-R diagrams of nearby galaxies by Humphreys (1981) with model O-star evolutionary tracks. The effect of changing the cutoff mass will be discussed later; the final derived SFRs turn out to be relatively insensitive to the cutoff for $50 \lesssim M_{upper} \lesssim 250\ M_\odot$.

Models were constructed for two other IMFs enriched in massive stars relative to the Miller-Scalo function. An "extended" Miller-Scalo function, with a constant slope $\psi(m) \propto m^{-2.5}$ above 1 $M_\odot$ was adopted; this IMF is very close to the well-known Salpeter (1955) IMF [$\psi(m) \propto m^{-2.35}$], and in the following discussion the extended IMF will be referred to as a Salpeter function for convenience. Finally, the effects of using a very shallow IMF, with $\psi(m) \propto m^{-2}$ above 1 $M_\odot$ was considered, although we shall see that this function generally fails to reproduce the observed Hα and color properties of disk galaxies.

Implicit in this approach is the assumption that the photoionization arises from normal OB stars following a non-pathological IMF. In particular we ignore the possibility that supermassive stars contribute significantly to the ionization. If such objects are present in large numbers, our whole statistical approach breaks down. One check on the method is to derive the model luminosities of the brightest blue stars as a function of the galaxy population, and then compare the results with the observed properties of nearby galaxies. Such a comparison is shown in Figure 2, where data on nearby galaxies from Sandage and Tammann (1982) are compared with the properties of model Sc galaxies [EW(Hα) = 25 Å] constructed according to the precepts described above, and scaled in proportion to galaxy luminosity. A mean $A_B = 1$ mag has been applied, in

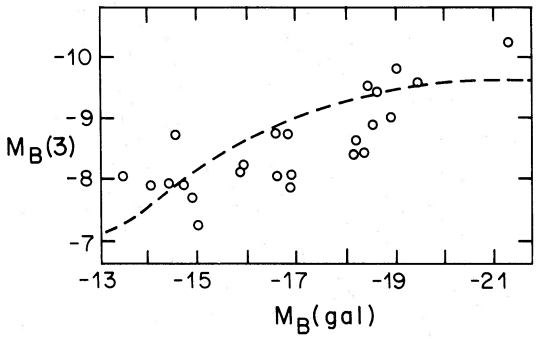

FIG. 2.—Mean absolute magnitude of the three brightest blue supergiants in nearby galaxies, from the compilation of Sandage and Tammann. The line represents the corresponding luminosity dependence of the three brightest blue stars in the model galaxies discussed in text. A mean absorption correction of 1 mag has been applied, in accordance with the extinction measurements of Humphreys in M33.

accordance with the reddening measurements of Humphreys (1980). The model and the observations are in reasonable agreement, but this does not necessarily imply that the model is correct in detail; the theoretical properties of the helium-burning supergiants used in generating the curve in Figure 2 are far too uncertain, and second order effects such as metallicity, dust, and IMF variations among the galaxies have been ignored. The general agreement does suggest, however, that our statistical approach is basically sound and is worth pursuing further.

IV. MODEL GALAXY COLORS: CONSTRAINTS ON THE IMF

The Hα photometry and the photoionization model described above can now be combined to yield estimates of the OB star formation rates in each program galaxy. These results are only mildly sensitive to the IMF slope adopted, since the mass range considered is relatively small ($\gtrsim 10\ M_\odot$), and because the contribution of each mass increment to the total UV luminosity is comparable. Any corresponding estimate of the *total* SFR, integrated over all stellar masses, is very sensitive to the adopted IMF, however, because of the large extrapolation involved; but by combining the Hα data with the broad-band *UBVR* properties of the galaxies we can place tight constraints on the IMF slope. The Hα emission is produced by massive (10–100 $M_\odot$) stars, while the red continuum in the galaxies is contributed primarily by low mass stars, mostly 0.7–3 $M_\odot$ red giants, so that the Hα equivalent width is a sensitive indicator of the IMF slope over that range of stellar mass.

In order to apply this constraint quantitatively, galaxy colors were modeled following the methods described by Tinsley (1972), Searle, Sargent, and Bagnuolo (1973), and Larson and Tinsley (1978). Evolutionary tracks for 0.8, 1.0, 1.25, 1.5, 2.25, 3, 5, 8, 10, 15, 20, 25, 30, 40, 50, 60, 80, and 100 $M_\odot$ stars were compiled from the literature (Iben 1965, 1966*a*, *b*, *c*, 1967*a*, *b*; Tinsley 1972; Chiosi, Nasi, and Sreenivasan 1978; Stothers and Chin 1979) and used with the Kurucz (1979) atmospheres to generate the *UBVR* luminosities as a function of time for each stellar mass. Data for stars of lower mass were taken from Tinsley and Gunn (1976); the massive star data were described earlier. Model galaxies were then constructed, using the IMFs listed earlier, a fixed age of 15×10^9 years (in accordance with the $H_0 = 50$ adopted earlier), and an exponentially declining star formation rate:

$$R(t) = R_0\, e^{-\beta t} \quad (0 \leq \beta \leq \infty)\,.$$

As such the models are virtually identical to those published by Searle, Sargent, and Bagnuolo (1973) and Larson and Tinsley (1978), except that here the upper end of the mass function is included so that ultraviolet fluxes could be calculated. The final models consisted of a grid of *UBVR* colors and Hα equivalent widths for each IMF, and for SFR decay times $\beta^{-1} = 0$, 1.5, 2, 3, 5, 7.5, 10, and 15×10^9 years, in addition to a model with constant star formation ($\beta = 0$) and a model with a linearly increasing SFR with time. The primary assumptions in these models have been discussed by Searle, Sargent, and Bagnuolo (1973). Most important are the assumption of a uniform and time-independent IMF and the neglect of reddening by dust.

Figure 3 displays the properties of the models in the two-color diagram. The three curves, one for each IMF, show the change in galaxy color from a linearly increasing SFR (blue end) to a purely 15×10^9 year old population (red end). Also plotted are the corrected colors of all spirals listed in the de Vaucouleurs, de Vaucouleurs, and Corwin (1976) catalog. Figure 3 simply confirms the previous conclusions of Searle, Sargent, and Bagnuolo (1973) and Larson and Tinsley (1978), that the observed colors of disk galaxies are well represented by a set of coeval models with varying SFR histories, and that the best fit to the *UBV* colors is for an IMF slope near Salpeter's original value. In detail these models cannot be correct, of course. Bulge light and dust are ignored, but since both of these effects tend to change the galaxy colors along vectors which are nearly parallel to the observed two color relation, they will not substantially alter the agreement observed in Figure 3.

The Hα equivalent widths are tightly correlated with the broad-band colors, and they place tighter constraints

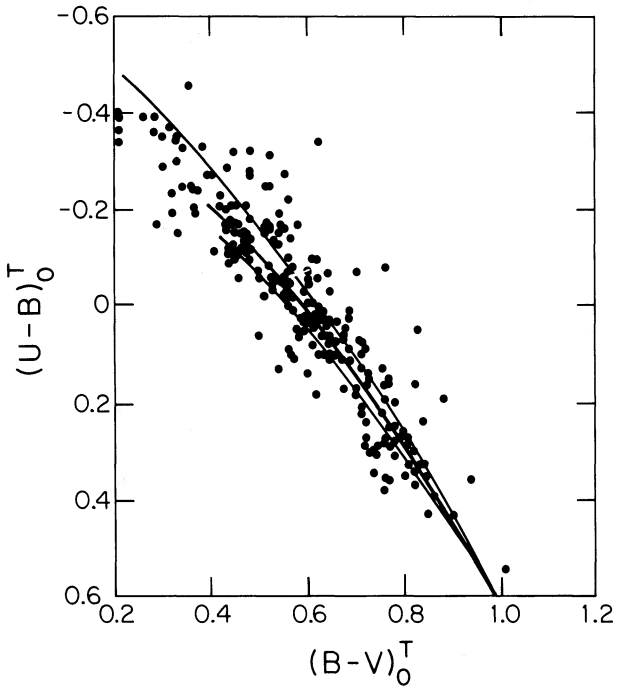

FIG. 3.—Two-color diagram from Shapley-Ames spiral galaxies, along with the model galaxy disk colors described in the text. The three curves correspond to the different mass functions adopted, the Miller and Scalo function (*lowest curve*), the extended Miller-Scalo (i.e., "Salpeter") function, and the shallow m^{-2} IMF (*top curve*).

on the range of IMF slopes in the disk galaxies. Model equivalent widths were calculated as follows:

$$\mathrm{EW(H}\alpha) = \frac{1.36 \times 10^{-12} N_{\mathrm{Lyman}}}{f_\lambda(6563\ \text{Å})},$$

$$\mathrm{EW(H}\alpha + [\mathrm{N\ II}]) = 1.33\mathrm{EW(H}\alpha).$$

The red continuum fluxes were calculated from the model R magnitudes, using the conversion given by Johnson (1966). The model Hα + [N II] equivalent widths and $B-V$ colors are plotted in Figure 4, for each of the three IMFs considered, along with the observed data from Paper I. In this case it is important to account for the effects of dust extinction on the Hα fluxes (see § II); this is shown schematically in Figure 4 by plotting the model (Hα, $B-V$) relations as areas whose upper bound represents the absorption-free model, and whose lower bound corresponds to a depression of a factor 2 (0.8 mag) in the equivalent width at the same color. Since the dust will affect both the Hα flux and the red continuum and $B-V$ colors (the latter to a lesser degree), it is not possible to precisely model the effect of the dust. The results in § II suggest, however, that the lower range of Hα model widths, corresponding to high selective extinction, are probably the most relevant.

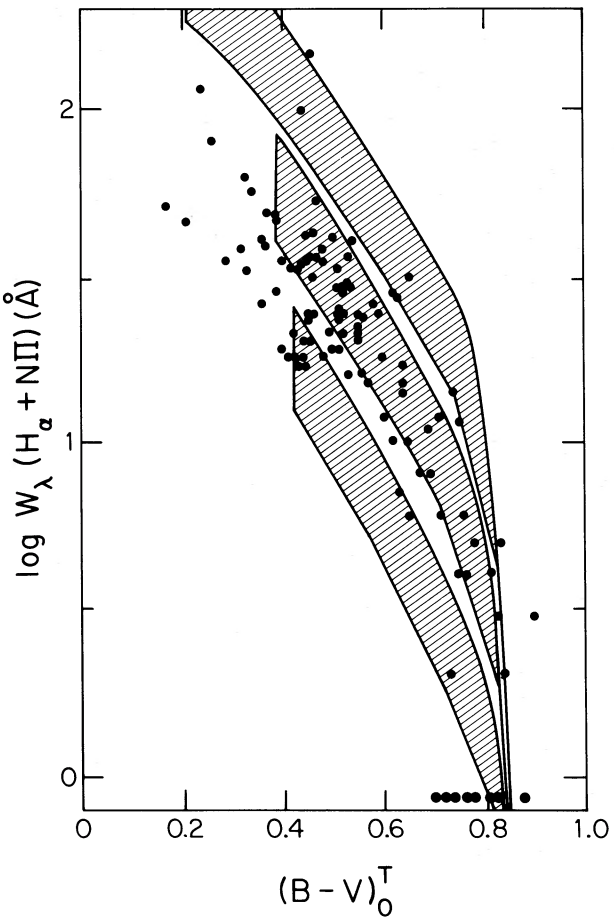

FIG. 4.—Observed emission line equivalent widths and corrected RC2 colors for observed galaxies, along with the evolutionary models. The effect of dust has been shown by plotting each model as an area, as described in the text. The IMFs corresponding to each model are the same as in Fig. 3.

As anticipated, the range in IMFs allowed by the data is quite narrow. Excluded in particular are the Miller-Scalo function, which produces 2–5 times too little emission, and the very shallow m^{-2} function, which produces 2–5 times too much, at least for galaxies in the color range $B-V \lesssim 0.7$ mag, where the Hα width is most sensitive to the IMF. The intermediate (Salpeter) IMF, however, seems to reproduce the observed galaxy properties very well, within the uncertainties introduced by absorption. As was seen in Figure 3 and in earlier work by Searle, Sargent, and Bagnuolo (1973) and Larson and Tinsley (1978), this same IMF best reproduces the observed UBV colors of disk galaxies. Hence a simple picture in which the present colors of (late-type) disk galaxies are determined by the star formation history is capable of reproducing the observed mean colors of galaxies, over a range of wavelength from the Lyman UV to 7000 Å. In practical terms this means that we can apply this constraint, and use the best fitting IMF to derive not only an OB SFR, but also a total SFR from the Hα photometry.

The failure of the Miller-Scalo solar neighborhood IMF to reproduce the observed galaxy colors should not be particularly disturbing. The high-mass end of the solar neighborhood function is only poorly determined, and Garmany, Conti, and Chiosi (1982) have found evidence for considerable variation in the local IMF slope. It is also worth noting that the Miller-Scalo function *is* capable of reproducing the colors of the red early-type spirals in Figures 3 and 4, though for those galaxies the disk evolution model given here is not strictly valid. In summary it is important to stress that the present observations suggest that the IMF in Sbc-Sc galaxies is shallower than in the solar neighborhood, but it is quite possible that the IMF is quite different in other types of galaxies. It should perhaps be noted that the Hα emission properties of the galaxy models shown in Figure 4 are sensitive to both the IMF slope and upper mass limit. The Miller-Scalo IMF can be brought into accord with the observations, but only if it extends well above 250 $M_\odot$, the limit of the available O-star tracks.

V. STAR FORMATION RATES

For the adopted initial mass function:

$$\psi(m) \propto m^{-1.4} \quad (0.1 \leq m \leq 1\ M_\odot)$$
$$\propto m^{-2.5} \quad (1 \leq m \leq 100\ M_\odot),$$

the relationship between the star formation rate and the Hα luminosity of a galaxy reduces to a single constant:

$$\mathrm{SFR}(\geq 10\ M_\odot) = \frac{L(\mathrm{H}\alpha)}{7.02 \times 10^{41}\ \mathrm{ergs\ s^{-1}}}\ M_\odot\ \mathrm{yr}^{-1},$$

$$\mathrm{SFR(total)} = \frac{L(\mathrm{H}\alpha)}{1.12 \times 10^{41}\ \mathrm{ergs\ s^{-1}}}\ M_\odot\ \mathrm{yr}^{-1}.$$

Total estimated star formation rates derived in this way are listed for the program galaxies in Table 1 in the Appendix. Again the reader is warned that the *individual* entries in the table probably possess uncertainties due to variable extinction of order $\pm 50\%$, independent of any systematic uncertainties in the SFR models. The derived total SFRs range from essentially zero in early-type galaxies, to as much as 10–20 $M_\odot$ yr^{-1} in giant Sc galaxies. The rates derived here are in excellent general agreement with the model SFRs derived in a quite different way by Larson, Tinsley, and Caldwell (1980), and the mean value of ~ 4 $M_\odot$ yr^{-1} found for Sb–Sbc galaxies in this sample is similar to that determined for our Galaxy by Smith, Biermann, and Mezger (1978).

The sensitivity of the derived SFR values on the presumed slope and cutoff mass of the IMF can easily be calculated, and scaling factors for other choices are listed in Table 2 in the Appendix. Most of these alternative combinations are inconsistent with the observed colors and Hα equivalent widths, however, as discussed above. One *can* force agreement with the observations with different choices of the IMF slope by altering the upper cutoff mass as well, for example by combining the steep Miller-Scalo function with a very high cutoff mass (>240 $M_\odot$). In such cases, however, the total SFR derived from the Hα flux is nearly the same as found earlier, because the reduction in the derived SFR resulting from the increased cutoff mass is almost exactly cancelled by the increase in the IMF slope. Hence within the broad range of IMFs and cutoff masses considered here, *the total star formation rates are relatively insensitive to the upper mass cutoff in the IMF*, if agreement with the observed galaxy colors is required.

The results in Tables 1 and 2 also illustrate the problems with a steep (e.g., Miller-Scalo) IMF in another way. For reasonable choices of the cutoff mass, say 60–150 $M_\odot$, the SFR values implied by the Hα fluxes and the Miller-Scalo function are extremely high, as high as 100–200 $M_\odot$ yr^{-1} in giant Sc galaxies. Such rates are simply inconsistent with the measured masses and ages of galaxies, and serve as a warning against the indiscriminate application of Galactic initial mass functions in calculations of star formation rates in other galaxies.

VI. TESTING THE SFR VALUES: MODEL GALAXY COLORS

Before interpreting the implications of the star formation rates derived here, we would like to make an independent check on the reliability of the absolute rates. Up to now we have only tested the consistency of the Hα to continuum colors (equivalent widths) with the broad-band colors. It is important to test the reliability of the overall *absolute* SFR scale, by synthesizing the galaxy colors from the star formation rates directly, and comparing the predictions with the observed colors of disk galaxies.

This was done in the following way: for each galaxy in Table 1 the present derived SFR can be compared to the past average SFR, the latter simply being the stellar mass of the disk divided by its age. The disk mass was obtained by multiplying the blue luminosity of the galaxy from Sandage and Tammann (1981) by the empirical mass-to-light ratios for galaxies of different type as compiled by Faber and Gallagher (1979). The Faber-Gallagher M/L ratios were corrected for the different absorption scheme used by Sandage and Tammann, and were normalized to the Nilson–de Vaucouleurs radius of the disk rather than to the Holmberg radius (following Fisher and Tully 1981), since the former is more characteristic of the radius of the active star-forming disk. (The latter correction is analogous to the correction for unseen matter required in the Larson-Tinsley models.) The ratio of the current (Hα) and past SFR values in each galaxy then defines the value of the e-folding constant β in the color evolution models discussed in § IV, which in turn defines the model $UBVR$ colors of the galaxy.

Predicted colors were derived in this way for all program galaxies with reliably measured star formation rates, and Figure 5 compares the $B-V$ model colors with the actual $(B-V)_0^T$ colors from de Vaucouleurs, de Vaucouleurs, and Corwin (1976). While the procedure is strictly valid only for disk-dominated (Sbc and later) galaxies, a few values for Sb galaxies are also plotted for comparative purposes (Fig. 5, *crosses*). Within the uncertainties involved in this procedure the agreement is quite good; if anything, the observed colors are bluer than predicted in the late-type galaxies, suggesting that the SFR values derived here may be slightly too low. The neglect of reddening in the models would work in the same direction as well. The good agreement between the predicted and observed colors suggests that it is very unlikely that we have overestimated the true star

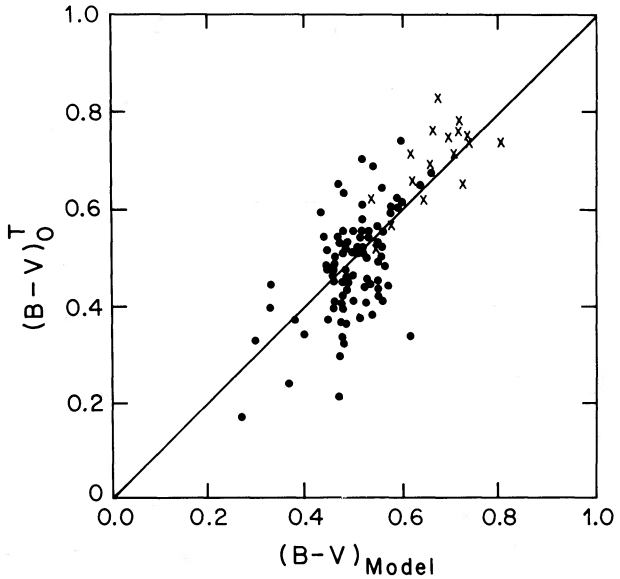

FIG. 5.—A comparison of the model $B-V$ galaxy colors, calculated from the star formation rates in Table 1, with the corrected RC2 colors of the galaxies. Points represent disk dominated galaxies, while the cross represent early (Sab–Sb) systems.

formation rates. If anything, the true rates may be slightly higher than those listed in the Appendix.

VII. DISCUSSION: IMPLICATIONS FOR GALAXY EVOLUTION

The star formation rates derived in § V are very high—high compared to the past rate of star formation in the galaxies, and high compared with the total amount of interstellar gas available for future star formation. Taken together, these results are difficult to reconcile with a traditional closed-system picture of galactic evolution, especially one in which the global SFR scales in proportion to a high power of the total gas content.

a) The Star Formation Histories

Figure 6 shows histograms of the ratio of the present SFR to the average past SFR in the program galaxies, as calculated in the last section. The most reliable results are for the well-sampled Sc galaxies; the Sb sample suffers from the insensitivity of Hα to low levels of star formation, while the few irregulars are heavily biased toward active star forming systems. The Hα-derived star formation rates confirm an earlier conclusion reached by Searle, Sargent, and Bagnuolo (1973), based on galaxy color models, that the present rate of star formation in late-type galaxies is comparable to the past rate averaged over the lifetimes of the disks. *Star formation has proceeded at relatively constant rate over the lifetimes of most late-type disk galaxies.* The early-type (Sa–Sb) spirals exhibit much lower values of $R_{\rm present}/\langle R\rangle$, but part of this arises because $\langle R\rangle$ includes past star formation in the bulge as well as the disk. If the Sab–Sb galaxies surveyed here possess bulge-to-disk ratios comparable to those measured by Boroson (1981), it is possible that the ratio of present to past SFR *in the disks* of the early-type galaxies is also of order unity. In other words, it is possible (though certainly not established) that the disks of all spiral galaxies may evolve at a relatively steady rate. At the other extreme, the results confirm Searle *et al.*'s conclusion that very blue galaxies $[(B-V)_0{}^T \lesssim 0.5$ mag] must have a present SFR that is higher than the past average rate, reflecting either a large transient burst of star formation or an average SFR that has been increasing over the lifetime of the disks.

The results in Figure 6 are difficult to reconcile with a picture in which the global star formation rate scales as the square (or some other high power) of the galaxy's total gas content. The power-law relation between the SFR and gas density ($R \propto \rho^n$, $n \approx 2$) derived by Schmidt (1959) is still widely applied, and it has been invoked by a number of investigators as a parameterization of the dependence of the total SFR in a galaxy on its total gas content. The present results are flatly inconsistent with such parameterizations. The total mass of interstellar gas in Sa–Sc galaxies is a small fraction of their total masses (typically 1–10%), and if the total SFR scales as the square of the gas content, such a model would predict initial disk SFRs 10^2–10^4 times higher than at present. Such SFR histories are clearly excluded by the results in Figure 6. While a power-law relationship between gas *density* and the SFR is not completely excluded by the present results (the mass and/or scale height of the galaxy disks may have evolved significantly over the disk lifetime), such changes are unlikely to erase the order-of-magnitude discrepancies between the observations and the implications of the Schmidt law. This apparent failure of the power-law relations to reproduce the observed SFR histories of galaxies is also

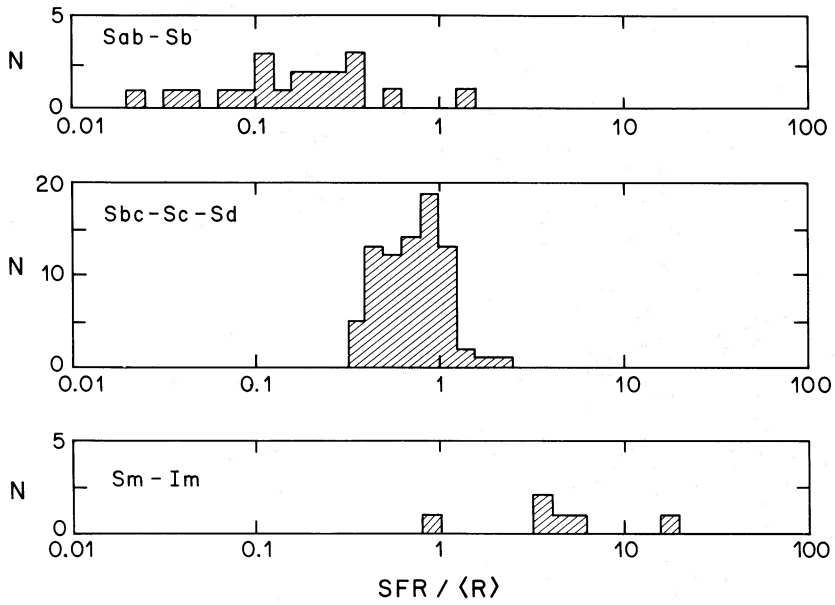

FIG. 6.—Distribution of current star formation rates, normalized to the average past rate in each galaxy. The small Sab–Sb and Sm–Im samples may be somewhat biased. The irregular galaxy sample is certainly biased toward active (bursting) star forming systems.

found in updated studies of the birthrate history of the solar neighborhood (Miller and Scalo 1979; Twarog 1980). The Galactic studies are only consistent with an $R \propto \rho^n$ power law if $n \ll 1$. Realistically, however, there is little observational support for any such parameterization at all. The global SFR might just as well be dictated by completely independent parameters, a result also suggested by the lack of any correlation between the total SFR and the total H I mass of galaxies (Hunter, Gallagher, and Rautenkranz 1982; Kennicutt and Kent 1983). Finally, we note that the observations reported here are inconsistent with a picture in which the SFR per unit nucleon in galaxies is a constant (Young and Scoville 1982*b*), because the SFR in the galaxies has remained relatively constant, despite the steady decrease in the amount of gas in the disks.

b) The Gas Depletion Time Scales

The present SFRs are also high when compared to the available supply of gas remaining in the galaxies. Figure 7 shows the distribution of depletion time scales for the galaxies in this study, obtained by dividing the available gas mass, as determined below, by the *present* SFR. The gas masses used in the calculations were obtained by multiplying each galaxy's total H I mass (Fisher and Tully 1981; Bottinelli, Gouguenheim, and Paturel 1982; Huchtmeier 1982, scaled in each case to $H_0 = 50$ km s^{-1} Mpc^{-1}) by a factor 2.0 to account for helium and molecular gas, and by 1.25 to account for recycled gas with this IMF, following Larson, Tinsley, and Caldwell (1980, hereafter LTC). The most uncertain factor is probably the H_2/H I ratio, and uncertainties in this correction will be discussed later.

The time scales in Figure 7 confirm the earlier model estimates of LTC and of Tinsley and Danly (1980). (The median LTC lifetime, obtained for a different sample of disk galaxies, is denoted by an arrow in Fig. 7.) The range in depletion times is large, probably reflecting both real variations and uncertainties in our necessarily simple-minded calculations, but most galaxies are consuming their interstellar gas at a rate which can only be sustained for another few billion years. Furthermore, since a major portion of the H I lies outside the star-forming disk in many of these galaxies, the inner disks may deplete their gas on even shorter time scales, depending to a large degree on how much molecular gas is present in those regions, and at what rate the H I may diffuse inward (Icke 1979).

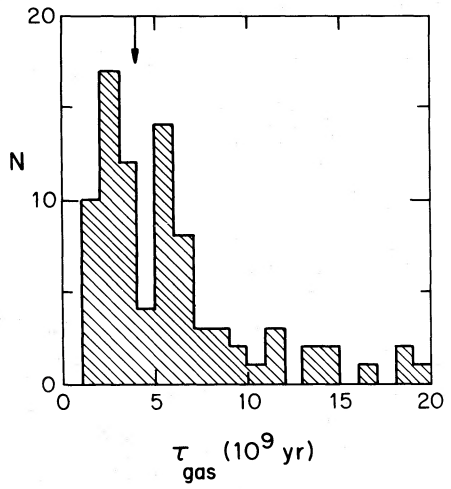

FIG. 7.—Current established time scales for consumption of the remaining interstellar gas in the program galaxies. The time scales include corrections for recycling and molecular gas. The arrow denotes the median consumption time scale derived for a different galaxy sample by Larson, Tinsley, and Caldwell, using color evolution models.

The two conclusions of this section taken together, that the disks of late-type galaxies have evolved relatively steadily in the past, but that this star formation must change radically in the next few billion years, is a surprising and an admittedly suspicious result. It is important to review the assumptions which were made along the way, and to consider any possible alternatives to this dilemma. Below we consider (and in many cases dismiss) the following possibilities in turn:

1. The Hα-derived star formation rates are systematically overestimated by a large factor, due to a systematic error in the photoionization model.
2. The remaining interstellar gas masses have been grossly underestimated, due to an underestimate of the molecular gas mass.
3. The galaxy sample studied is inadvertently biased toward unusually active star-forming galaxies; their time-averaged SFRs are much lower.
4. The average IMF in galaxies is radically different from the measured in the solar neighborhood, in the sense that we have grossly overestimated the number of low-mass stars being formed. This explanation has been proposed by Talbot (1980) and by Jensen, Talbot, and Dufour (1981).
5. The time scale calculations are correct, but the interstellar gas is being constantly replenished by infalling gas from outside.
6. The time scale calculations are correct. Infall is a minor effect. We live in an epoch characterized by relatively rapid changes in galaxy properties.

The consistency of the Hα-derived star formation rates with the observed broad-band colors of the galaxies, and the agreement of the consumption time scales derived here with those of LTC, suggest that the Hα SFR results cannot suffer from gross systematic errors. If anything, the Hα flux probably underestimates the total SFR, since a small fraction of the Lyman continuum radiation probably escapes from the galaxy. Reddening of the broad-band colors by dust, not taken into account in either set of models, would also lead to underestimates of the true SFR. There is little evidence supporting the contention that the SFRs in this paper are too large. If anything, they may be too low.

A second source of error might be the molecular gas corrections used in the calculations here. CO data are now available for a large number of galaxies, mainly as a result of the efforts of the Massachusetts–Stony Brook group, but considerable controversy

surrounds the determination of total molecular gas densities from the CO line fluxes. Estimates of $M(H_2)/M(H\ I)$ in galaxies range from 0.15 (Morris and Lo 1978) to ~ 1 (Young and Scoville 1982*a*). If we adopt the upper limit of these estimates, then the time scales in Figure 6 would increase by 30–40% at most. The question of the molecular mass is most important for the consumption time scales in the inner region of galaxies, but not for the overall time scales.

If the galaxy sample selected for Hα photometry represents unusually active objects, then the derived time scales for gas consumption would be unrealistically short. While a slight bias may be present in this sample, it is certainly not large. The Hα sample is a large one, and it represents a diverse range of galaxy morphologies, colors, and gas contents. The primary selection criterion was that the galaxies possess published colors in the de Vaucouleurs *et al.* RC2 catalog. Tinsley and Danly (1980) have investigated the color distribution of the RC2 galaxy sample for the expressed purpose of testing for such a selection effect, and concluded that the sample is representative. Except for an intentional bias in the Hα measurements toward late-type galaxies, the present sample is a representative cross section in turn of the RC2 sample. While there clearly exist low surface brightness spirals (Romanishin 1980) with gas consumption lifetimes which are likely to be considerably larger than a Hubble time, such galaxies appear to be very rare (Thuan and Seitzer 1979). The only other conceivable bias might be that the Sc galaxies as a class represent "flashing" galaxies. In this scenario, offered by a colleague who prefers to remain anonymous, spirals could exhibit periodic star formation bursts; during bursts they would be classified as Sc's, while between bursts they would presumably be classified as S0–Sb galaxies. Thus the short depletion of time scales in Figure 7 would arise from the bias in my sample toward Sc galaxies. I find this an untenable explanation, however, because the galaxies in Figure 7 include Sab–Sb galaxies as well as Sc's, and because the morphological and dynamical differences between different types of galaxies along the Hubble sequence appear to limit the degree to which a given galaxy could evolve from one type to another.

Talbot (1980) and Jensen, Talbot, and Dufour (1981) derived a similarly short gas consumption time scale in their study of M83, and suggested as an alternative that the IMF there may be radically different from a Salpeter or a Miller-Scalo function. In particular they suggested that two mechanisms of star formation are present, one forming predominantly massive stars, the other only low-mass stars, with the massive mode dominating at present in the galaxy. If this interpretation were correct, the SFRs in this paper would be systematically high. In order to investigate the effects of such a bimodal IMF on the Hα emission and colors of galaxies, evolutionary models were run with normal Salpeter and Miller-Scalo IMFs over the first 10^{10} years, but with IMFs truncated below a mass M_L over the past 5×10^9 years. The Hα emission and colors for one such set of models, with the "Salpeter" IMF truncated below masses of 10 $M_\odot$ (the limit suggested by Talbot and by Jensen *et al.*), 3 $M_\odot$, and 1 $M_\odot$, are shown in Figure 8. The 10 $M_\odot$ and 3 $M_\odot$ models are clearly inconsistent with the observed colors with an IMF truncated below 1 $M_\odot$ (especially the lack of 1–10 $M_\odot$ giants. It is possible to marginally reproduce the observed colors of galaxies with a present IMF truncated below 1 $M_\odot$ (especially if the RC2 colors were systematically too blue); but since 60–70% of the mass in the total IMF is from stars above 1 $M_\odot$, truncating the IMF at 1 $M_\odot$ only lowers the derived SFRs slightly. Such a scenario would also have to contend with the observed preponderance of low-mass stars in the solar-neighborhood IMF. Finally, it should be noted that the specific IMF offered by Jensen *et al.* for M83, namely one which favors almost exclusively the formation of stars in the 10–30 $M_\odot$ range (types O7–B3), is even more untenable for the present galaxy sample. Terminating the IMF at 30 $M_\odot$ severely diminishes the Lyman continuum emission of the

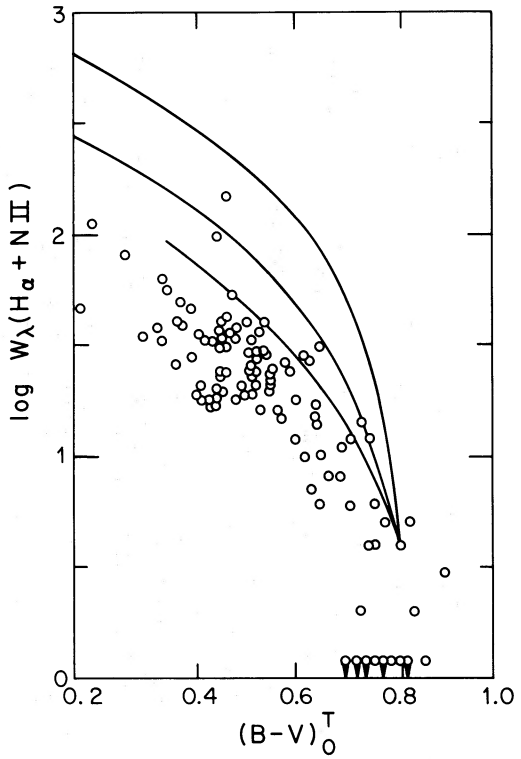

FIG. 8.—Hα-color relation for model galaxies with initial mass functions which are depleted in low mass stars. The three curves shown correspond to models with two IMF components, a normal Salpeter function and a second IMF which terminates below a cutoff mass of 10 $M_\odot$ (*upppr*), 3 $M_\odot$ (*middle*), and 1 $M_\odot$ (*lower curve*). The curves were generated by varying the mixing ratio of the two components (details in the text). The points are the observed galaxy properties. Note that the curves do not include the effects of absorption by dust; the effect of dust is probably different than shown in Fig. 4; but the absorption-corrected curves may be as much as a factor 2 lower than shown. This is still much smaller than the discrepancy between the 10 $M_\odot$ and 3 $M_\odot$ curves and the observed points.

stellar population, and the SFRs which would be implied by such an IMF are only 2–3 times smaller than those listed in Table 1, and *all* in O7–B3 stars! A typical ScI galaxy would be forming 5–10 $M_\odot$ yr^{-1} in O7–B3 stars alone, and would presumably produce a Type II supernova every 1–3 years. While such extreme IMFs may not offer valid alternatives to the more conventional mass functions used in this paper, the examples do illustrate the degree to which the derived SFRs and assumed IMFs are coupled in these observations, and they emphasize the need for independent measurements of IMFs in other galaxies.

In summary, we see that while uncertainties in the assumptions which underlie the star formation and depletion rates may certainly influence the results at the 50% level, it is difficult to extend the galaxy lifetimes by much more than that. The consistency of the star formation histories found in three independent sets of studies, the present Hα results, the broad-band modeling of the Yale group, and the solar neighborhood studies of Miller, Scalo, and Twarog, strongly constrains the range of possible alternatives—it is difficult to construct a series of systematic effects that would alter all three methods in the same way.

c) *Evidence for Infall or Rapid Galaxy Evolution*?

If the time scales in Figure 7 are correct, then the majority of nearby galaxies will change rapidly in the next 2–6 × 10^9 years, unless the gas disks are replenished from outside. Infall has been suggested by a number of investigators, including LTC, as a solution to both the depletion "problem" and in order to explain the chemical enrichment histories of galactic disks (Audouze and Tinsley 1976). Infall may offer an attractive solution to the gas consumption dilemma in Sa–Sb galaxies, but it does not work as well for the late-type spirals. In the Sa–Sb systems the star formation rates are low, typically a few solar masses per year, and such depletion rates can be sustained by recycling and by a modest rate of accretion, either diffuse gas or captures of gas-rich companion galaxies (LTC). In the Sc galaxies, however, the depletion rate is much higher (up to 10–20 $M_\odot$ yr^{-1}), and this rate has been sustained over the history of the disks. Maintaining such an appetite would require that the galaxies accrete 5–10% of their mass every 10^9 years. Infall in such a context would no longer constitute a second-order phase of galaxy evolution; it would require that a major stage of galaxy formation is still taking place. While infall on such a scale probably cannot be excluded observationally, it raises serious dynamical and evolutionary questions. Why, for instance, does the intergalactic gas prefer to fall in greater quantities on to the small-bulge, slowly rotating Sc systems? Nevertheless, while it is difficult to understand how infall could replenish all of the gas being expended in the Sc galaxies, moderate amounts could certainly extend their star-forming lifetimes significantly.

Finally, we should consider the results in Figure 7 at face value, without infall, without systematic errors, without unusual IMFs, and with the possibility that many galaxies will exhaust most of their interstellar gas in the new few billion years. The median time scale in Figure 7 is considerable, 25–40% of the Hubble time; and if the SFR in the future drops in these galaxies, the "burnout" times will be even longer, so the time scales derived here are really not that short. Butcher and Oemler (1978) report a pronounced difference in galaxy populations in rich clusters at look-back times of 3–5 × 10^9 years, suggesting that rapid color evolution may have already occurred in at least some of the spirals in rich clusters, and our own data on the Coma cluster suggest that the few spirals which remain there may exhaust their remaining gas in a very short time as well (Kennicutt, Bothun, and Schommer 1983). Sa galaxies in the field (and perhaps some of the S0's) may be examples of galaxies which have already reached this stage.

Whatever the explanation for these results, it seems clear that at least some of the widely held assumptions concerning the evolution of disk galaxies must be fundamentally modified. Either galaxies do not evolve as closed systems, or else we must abandon the idea that a galaxy's appearance, gaseous and stellar contents, and position on the Hubble sequence (in terms of disk resolution and disk/bulge morphology) are immutable properties over 10^9 year time scales. It is possible that both assumptions are incorrect. Radical changes in the IMF may account for some of the observations, but probably not all of them, and such changes in themselves would force a serious rethinking of our traditional approach to modeling galaxy evolution. Finally, the idea that the global SFR is a simple one-parameter function of the mean gas content in a disk galaxy has found little observational support here, though it still may be valid as a local law. The uncertainties and paradoxes raised by these results are symptomatic of the observational immaturity of the field; hopefully more detailed observations of both the SFR's and IMFs in galaxies will provide some answers.

VIII. SUMMARY

1. The integrated Balmer line emission from a galaxy can be used as a direct probe of its current star formation activity. The primary observational limitation is extinction by dust, but radio continuum measurements can be used to correct for the extinction on average.

2. The photoionization properties of a population of massive stars have been calculated for various initial mass functions. Together with the Hα photometry they enable reasonably accurate (±30%) estimates of the massive SFR to be made in a large sample of galaxies.

3. The equivalent width of the Hα emission line is very sensitive to the IMF slope between 1 and 50 $M_\odot$. Simple evolutionary models of the type studied by Searle, Sargent, and Bagnuolo (1973) and Larson and Tinsley (1978) reproduce both the *UBVR* and the Hα properties of spiral galaxies if a Salpeter IMF is used. The range of permitted IMFs is small. The Miller-Scalo solar neighborhood IMF does not reproduce the observed

TABLE 1

Hα Fluxes and Derived Star Formation Rates

NGC	Type	$-M_B^{0,i}$	EW(Hα + N II) (Å)	log F_c(Hα) (ergs s^{-1})	SFR ($M_\odot$ yr^{-1})
357	SBa	21.1	-1 ± 3	...	...
718	Sa	20.5	-3 ± 3	...	...
1079	Sa	21.0	-1 ± 2	...	...
1291	SBa	21.7	1 ± 3	...	...
1302	Sa	21.2	2 ± 2	...	...
1357	Sa	21.1	5 ± 2	41.2:	1.4:
2681	Sa	20.5	-2 ± 2	...	...
2775	Sa	20.8	1 ± 1	...	...
3623	Sa	21.5	1 ± 1	...	...
4274	Sa	20.9	4 ± 4	...	...
4866	Sa	21.1	-2 ± 3	...	...
6340	Sa	21.1	0 ± 2	...	...
7213	Sa	22.0	1 ± 2	...	...
7743	SBa	21.0	3 ± 3	...	...
488	Sab	22.9	1 ± 1	...	...
681	Sab	20.8	4 ± 2	...	...
3368	Sab	21.4	5 ± 2	41.20	1.4
4594	Sab	22.8	2 ± 1	...	...
4736	Sab	20.8	8 ± 1	41.21	1.4
7177	Sab	21.1	6 ± 2	41.12	1.0
7716	Sab	21.3	10 ± 2	41.51	2.7
1832	SBb	21.5	28 ± 3	41.91	7.0
2841	Sb	21.5	2 ± 2	...	($\leq$0.5)
3351	SBb	20.7	12 ± 2	41.27	1.6
3521	Sb	21.7	14 ± 2	41.65:	3.8:
3627	Sb	21.5	18 ± 1	41.60:	3.5:
5746	Sb	22.6	12 ± 4	41.75	4.9
5806	Sb	20.2	15 ± 4	41.24	1.5
7217	Sb	21.7	6 ± 2	41.51	2.7
7723	SBb	21.8	10 ± 2	41.61	3.5
I5271	Sb	20.7	14 ± 4	40.92	0.8
150	Sbc	21.3	24 ± 2	41.77:	5.1:
278	Sbc	20.7	36 ± 2	41.76	4.9
3310	Sbc	20.8	113 ± 4	42.15	12.2
4666	Sbc	21.5	31 ± 2	42.04	9.7
5033	Sbc	21.1	17 ± 2	41.60:	3.5:
5055	Sbc	21.3	15 ± 1	41.65:	3.8:
5194	Sbc	21.6	24 ± 2	41.95:	7.6:
5248	Sbc	21.2	21 ± 1	41.71:	4.3:
5970	SBbc	21.4	24 ± 5	42.15	12.4
6217	SBbc	21.1	29 ± 2	41.81	5.4
6574	Sbc	21.3	27 ± 5	41.94	7.6
7392	Sbc	21.7	11 ± 4	41.85	6.2
7479	SBbc	22.3	12 ± 3	41.98:	8.1:
157	Sc	22.2	28 ± 2	42.18	13.2
337	Sc(p)	21.1	49 ± 4	41.97	8.1
428	Sc	20.6	18 ± 3	41.38	2.0
450	Sc	20.7	38 ± 4	41.68	4.1
628	Sc	21.8	24 ± 2	41.99	8.4
672	SBc	19.9	20 ± 3	41.06	1.0
949	Sc	19.8	21 ± 3	41.04	1.0
1058	Sc	19.3	21 ± 3	40.86	0.6
1073	SBc	20.9	20 ± 3	41.49	2.7
1084	Sc	21.6	41 ± 2	42.15	12.1
1087	Sc	21.4	35 ± 3	41.97	8.1
1232	Sc	22.6	20 ± 3	42.32:	17.8:
1385	Sc	21.8	46 ± 2	42.21	14.0
1518	Sc	19.4	33 ± 4	41.15	1.2
1637	Sc	19.7	16 ± 2	41.02	0.9
2139	SBc	21.2	46 ± 3	41.91	7.0
2276	Sc	22.1	42 ± 4	42.35	19.4
2763	Sc	20.5	29 ± 2	41.53	3.0
3389	Sc	19.9	35 ± 4	41.32	1.8
3486	Sc	20.1	35 ± 4	41.41	2.2
3631	Sc	21.3	30 ± 3	41.87	6.5

TABLE 1—*Continued*

NGC	Type	$-M_B^{0,i}$	EW(Hα + N II) (Å)	log F_c(Hα) (ergs s^{-1})	SFR ($M_\odot$ yr^{-1})
3726	Sc	20.7	17 ± 3	41.41	2.2
3810	Sc	20.2	36 ± 3	41.57	3.2
3938	Sc	20.5	24 ± 3	41.53	3.0
4027	Sc	21.1	31 ± 7	41.82	5.7
4152	Sc	20.9	33 ± 8	41.77	5.1
4303	Sc	21.8	34 ± 3	42.22:	14.0:
4420	Sc	20.2	40 ± 5	41.54	3.0
4487	SBc	19.8	21 ± 5	40.96	0.8
4496	SBc	20.4	33 ± 5	41.38	2.1
4504	Sc	19.5	27 ± 5	41.03	0.9
4536	Sc	22.2	18 ± 4	41.94	7.8
4597	SBc	19.1	37 ± 8	41.02	0.9
4602	Sc	21.7	17 ± 6	41.71	4.5
4631	Sc	21.4	39 ± 3	41.85	6.2
4632	Sc	20.9	34 ± 3	41.68	4.1
4658	SBc	21.1	19 ± 7	41.53	3.0
4713	SBc	19.9	56 ± 3	41.71	4.4
4775	Sc	20.8	37 ± 3	41.59	3.2
4781	Sc	19.6	25 ± 7	41.03	1.0
4808	Sc	18.5	43 ± 7	40.95	0.8
4900	Sc	19.0	40 ± 4	41.31	1.8
5364	Sc	21.2	16 ± 2	41.64:	3.8:
5676	Sc	22.1	22 ± 2	42.08	10.3
5962	Sc	21.3	24 ± 2	41.86	6.2
6015	Sc	20.5	33 ± 3	41.6:	3.2
6070	Sc	21.2	25 ± 5	41.79:	5.1:
6106	Sc	20.1	41 ± 7	41.53	3.0
6181	Sc	21.6	38 ± 3	42.16	12.4
6207	Sc	20.0	35 ± 4	41.40	2.2
6412	SBc/Sc	20.6	21 ± 3	41.47	2.5
6503	Sc	18.8	19 ± 2	40.65:	0.4
6643	Sc	21.6	33 ± 2	42.04	9.5
6946	Sc	20.3:	29 ± 5	41.4:	3.5:
7137	Sc	20.4	24 ± 4	41.59	3.2
7218	Sc	20.7	26 ± 4	41.67	4.1
7448	Sc	22.0	40 ± 4	42.21	14.0
7590	Sc	20.8	53 ± 3	41.85	6.2
7741	SBc	20.2	24 ± 2	41.31:	1.8
2976	Sd	17.5	26 ± 2	40.21	0.15
3955	S(p)	20.0	19 ± 4	41.12	1.0
4790	Sd	19.4	30 ± 3	41.15	1.2
5204	Sd	18.1	28 ± 2	40.57	0.3
5474	Scd	18.4	18 ± 2	40.45	0.25
5585	Sd	18.5	18 ± 4	40.44	0.25
1156	Sm	18.3	99 ± 20	40.85	0.6
1569	Sm	16.2:	149 ± 15	40.7:	0.4
4214	SBm	18.8	47 ± 3	41.1	1.1
4449	Sm	18.8	63 ± 1	41.2	1.4
7764	SBm	20.1	35 ± 4	41.5	2.6
I4662	Im	17.2	51 ± 11	40.7:	0.4

properties of late-type spirals, unless the IMF extends to extremely high masses. The present models are not sensitive enough to place meaningful constraints on the IMF in early type systems.

4. The total star formation rates derived from the Hα photometry range from 0 to 20 $M_\odot$ yr^{-1}. The star formation rates derived for individual galaxies have been used to calculate model colors, and the predicted colors are in good general agreement with the measured colors of the galaxies, indicating that any systematic errors in the SFR scale are probably at the ±50% level or less. If anything, the true SFR values may be somewhat higher than determined here. Altering the distance scale used changes the absolute SFRs, but not the qualitative conclusions summarized below.

5. The present rate of star formation in late type spiral and irregular galaxies is comparable to the average past rate in the disks. This probably excludes a global star formation rate which is porportional to a high power ($n > 1$) of the average gas density. This

general result corroborates the conclusion derived from solar neighborhood studies by Miller and Scalo (1979) and by Twarog (1980). It does not confirm the recent conjecture of Young and Scoville (1982*b*), based on the CO content and blue magnitudes of a few nearby spirals, that the SFR per unit nucleon is constant in galaxies.

6. The gas consumption time scales represented by the derived SFRs are short, typically a few times 10^9 years for all types of spiral galaxies, in good general agreement with the estimates of Larson, Tinsley, and Caldwell (1980). Infall of fresh gas or an evolving IMF may lengthen the time scale, but neither effect appears capable of changing it by more than about a factor of 2. The evidence suggests that we may live in an epoch of relatively rapid gas depletion and evolution in disk galaxies.

7. All of the above must be qualified with a summary of the systematic uncertainties which may still plague the SFR determinations. Particularly vexing are the effects of dust, both on the line emission and on the broad-band colors, the uncertain role of very high mass stars, the role of very low mass stars, and the possibility of large IMF variations, either among galaxies or as a function of time within galaxies.

The photometry used in this study was obtained while I held a postodoctoral fellowship at the Mount Wilson and Las Campanas Observatories, Carnegie Institution of Washington. Their support and generous allocation of telescope time is most gratefully acknowledged. The data reduction and analysis were supported by a summer research fellowship from the University of Minnesota Graduate School and by the NSF through grant AST 81-11711. I would especially like to extend thanks to Thijs van der Hults, Frank Israel, and Ule Klein for providing their unpublished radio data, and to the staff at Leiden University for their hospitality while this paper was being written.

TABLE 2

SCALING FACTORS FOR OTHER IMFs[a]

IMF	MAXIMUM MASS ($M_\odot$)			
	30	60	100	200
Miller-Scalo	8.01	4.05	3.35	2.55
Extended M-S	3.78	1.44	1.00	0.53
Shallow	1.44	0.43	0.26	0.11

[a] Most alternatives are inconsistent with observed galaxy colors and Hα emission (see text).

APPENDIX

RESULTS FOR INDIVIDUAL GALAXIES

Listed in Table 1 are individual Hα fluxes and derived total star formation rates for the program galaxies. The sample is the same as surveyed by Kennicutt and Kent (1983), except that galaxies with strong nuclear emission and Virgo cluster members have been excluded. Fluxes are not listed for galaxies with marginally detected emission. Absolute "corrected" Hα fluxes are based on an $H_0 = 50$ km s^{-1} Mpc^{-1} distance scale, and mean [N II] and extinction corrections as described in the text. Note that variable extinction probably introduces uncertainties on the order of ± 30–50% in the Hα fluxes and star formation rates of individual galaxies. The star formation rates listed in the last column of Table 1 refer to *total* rates, down to 0.1 $M_\odot$, and are based on the "extended" Miller-Scalo function described in the text. Rates derived using a Salpeter (1959) IMF would be virtually identical. Again I stress that individual entries in Table 1 must be applied conservatively; the list has been included in order to provide a more quantitative picture of the magnitude and the variability of the star formation rates in galaxies of different types.

Table 2 lists the factors by which the rates in Table 1 should be scaled for different choices of IMF slope and cutoff mass. Note that most of these alternative choices are inconsistent with the observed galaxy colors and Hα + [N II] equivalent widths.

REFERENCES

Audouze, J., and Tinsley, B. M. 1976, *Ann. Rev. Astr. Ap.*, **14**, 43.
Balick, B., and Sneden, C. 1976, *Ap. J.*, **208**, 336.
Boroson, T. 1981, *Ap. J. Suppl.*, **46**, 77.
Bottinelli, L., Gouguenheim, L., and Paturel, G. 1982, *Astr. Ap. Suppl.*, **47**, 171.
Brocklehurst, M. 1971, *M.N.R.A.S.*, **153**, 471.
Burcher, H., and Oemler, A. 1978, *Ap. J.*, **219**, 18.
Chiosi, C., Nasi, E., and Sreenivasan, S. R. 1978, *Astr. Ap.*, **63**, 103.
de Vaucouleurs, G., de Vaucouleurs, A., and Corwin, H. G. 1976, *Second Reference Catalog of Bright Galaxies* (Austin: University of Texas Press).
Faber, S. M., and Gallagher, J. S. 1979, *Ann. Rev. Astr. Ap.*, **17**, 135.
Fisher, J. R., and Tully, R. B. 1981, *Ap. J. Suppl.*, **47**, 139.
Garmany, C. D., Conti, P. S., and Chiosi, C. 1982, *Ap. J.*, **263**, 777.
Gioia, I. M., Gregorini, L., and Klein, U. 1982, *Astr. Ap.*, **116**, 164.
Huchtmeier, W. K. 1982, *Astr. Ap.*, **110**, 121.
Hummer, D. G., and Mihalas, D. 1970, *M.N.R.A.S.*, **147**, 339.
Humphreys, R. M. 1980, *Ap. J.*, **241**, 587.
———. 1981, in *The Most Massive Stars*, ed. S. D'Odorico, D. Baade, and K. Kjar (Garching: ESO), p. 5.
Hunter, D. A., Gallagher, J. S., and Rautenkranz, D. 1982, *Ap. J. Suppl.*, **49**, 53.
Iben, I. 1965, *Ap. J.*, **142**, 1447.
———. 1966*a*, *Ap. J.*, **143**, 483.
———. 1966*b*, *Ap. J.*, **143**, 505.
———. 1966*c*, *Ap. J.*, **143**, 516.
———. 1967*a*, *Ap. J.*, **147**, 624.
———. 1967*b*, *Ap. J.*, **147**, 650.

Icke, V. 1979, *Astr. Ap.*, **78**, 21.
Israel, F. P., and Kennicutt, R. C. 1980, *Ap. Letters*, **21**, 1.
Israel, F. P., and van der Hulst, J. M. 1982, preprint.
Jensen, E. B., Talbot, R. J., and Dufour, R. J. 1981, *Ap. J.*, **243**, 716.
Johnson, H. L. 1966, *Ann. Rev. Astr. Ap.*, **4**, 193.
Keel, W. 1982, Ph.D. thesis, University of California, Santa Cruz.
Kennicutt, R. C., Bothun, G., and Schommer, R. 1983, in preparation.
Kennicutt, R. C., and Kent, S. M. 1983, *A.J.*, submitted (Paper I).
Kurucz, R. L. 1979, *Ap. J. Suppl.*, **40**, 1.
Larson, R. B., and Tinsley, B. M. 1978, *Ap. J.*, **219**, 46.
Larson, R. B., Tinsley, B. M., and Caldwell, C. N. 1980, *Ap. J.*, **237**, 692 (LTC).
Maeder, A. 1980, *Astr. Ap.*, **92**, 101.
Miller, G. E., amd Scalo, J. M. 1979, *Ap. J. Suppl.*, **41**, 513.
Morris, M., and Lo, K. Y. 1978, *Ap. J.*, **223**, 803.
Romanishin, W. 1980, Ph.D. thesis, University of Arizona.
Salpeter, E. E. 1955, *Ap. J.*, **121**, 161.
Sandage, A., and Tammann, G. A. 1981, *A Revised Shapley-Ames Catalog of Bright Galaxies* (Washington: Carnegie Institution of Washington Pub. 635).
———. 1982, in *Cosmology and Fundamental Physics* (Rome: Vatican Observatory).
Sarazin, C. L. 1977, *Ap. J.*, **211**, 772.
Schmidt, M. 1959, *Ap. J.*, **129**, 243.
Searle, L., Sargent, W. L. W., and Bagnuolo, W. G. 1973, *Ap. J.*, **179**, 427.
Smith, L. F., Biermann, P., and Mezger, P. G. 1978, *Astr. Ap.*, **66**, 65.
Stark, A. A. 1979, Ph.D. thesis, Princeton University.
Stothers, R., and Chin, C. W. 1976, *Ap. J.*, **204**, 472.
———. 1979, *Ap. J.*, **233**, 267.
Talbot, R. J. 1980, *Ap. J.*, **235**, 821.
Thuan, T. X., and Seitzer, P. O. 1979, *Ap. J.*, **231**, 680.
Tinsley, B. M. 1972, *Astr. Ap.*, **20**, 383.
———. 1981, *Ap. J.*, **250**, 758.
Tinsley, B. M., and Danly, L. 1980, *Ap. J.*, **242**, 435.
Tinsley, B. M., and Gunn, J. E. 1976, *Ap. J.*, **203**, 52.
Twarog, B. A. 1980, *Ap. J.*, **242**, 242.
Van Citters, G. W., and Morton, D. C. 1970, *Ap. J.*, **161**, 695.
Weedman, D. W., Feldman, F. R., Balzano, V. A., Ramsey, L. W., Sramek, R. A., and Wu, C. C. 1981, *Ap. J.*, **248**, 105.
Young, J. S., and Scoville, N. 1982*a*, *Ap. J.*, **258**, 467.
———. 1982*b*, *Ap. J.* (*Letters*), **260**, L11.

ROBERT C. KENNICUTT, JR.: University of Minnesota, Department of Astronomy, 116 Church Street, S.E., Minneapolis, MN 55455